

## Phototrophy and starvation-based induction of autophagy upon removal of Gcn5-catalyzed acetylation of Atg7 in *Magnaporthe oryzae*

Shulin Zhang<sup>a,b,†</sup>, Meiling Liang<sup>a,b,†</sup>, Naweed I. Naqvi<sup>c</sup>, Chaoxiang Lin<sup>a,b</sup>, Wanqiang Qian<sup>d</sup>, Lian-Hui Zhang<sup>a,b</sup>, and Yi Zhen Deng<sup>a,b</sup>

<sup>a</sup>Key Laboratory for Conservation and Utilization of Subtropical Agro-Bioresources, College of Agriculture, South China Agricultural University, Guangzhou, China; <sup>b</sup>Guangdong Province Key Laboratory of Microbial Signals and Disease Control, and Integrative Microbiology Research Centre, South China Agricultural University, Guangzhou, China; <sup>c</sup>Temasek Life Sciences Laboratory, and Department of Biological Sciences, National University of Singapore, Singapore; <sup>d</sup>The New Countryside Development Institute of South China Agricultural University, Guangzhou, China

### ABSTRACT

*Magnaporthe oryzae*, the ascomycete fungus that causes rice blast disease, initiates conidiation in response to light when grown on Prune-Agar medium containing both carbon and nitrogen sources. Macroautophagy/autophagy was shown to be essential for *M. oryzae* conidiation and induced specifically upon exposure to light but is undetectable in the dark. Therefore, it is inferred that autophagy is naturally induced by light, rather than by starvation during *M. oryzae* conidiation. However, the signaling pathway(s) involved in such phototropic induction of autophagy remains unknown. We identified an *M. oryzae* ortholog of *GCN5* (*MGG\_03677*), encoding a histone acetyltransferase (HAT) that negatively regulates light- and nitrogen-starvation-induced autophagy, by acetylating the autophagy protein Atg7. Furthermore, we unveiled novel regulatory mechanisms on Gcn5 at both transcriptional and post-translational levels, governing its function associated with the unique phototropic response of autophagy in this pathogenic fungus. Thus, our study depicts a signaling network and regulatory mechanism underlying the autophagy induction by important environmental clues such as light and nutrients.

### ARTICLE HISTORY

Received 9 October 2015  
Revised 11 April 2017  
Accepted 25 April 2017

### KEYWORDS

Atg7; autophagy; conidiation; Gcn5; histone acetyltransferase (HAT); *Magnaporthe oryzae*

### Introduction


Rice-blast disease caused by the filamentous ascomycete *M. oryzae* is responsible for significant crop losses globally and annually.<sup>1</sup> *M. oryzae* forms aerial hyphae (the hyphae that grow perpendicular into the air from the vegetative mycelial mat), when grown in darkness; whereas conidiation, formation of asexual spores, is initiated in response to light exposure.<sup>2</sup> These fungal asexual spores known as conidia are the key determinant of the spread and severity of blast disease as they can be easily dispersed and transmitted by air.<sup>3</sup> Functional analysis of several autophagy genes in *M. oryzae*, including *MoATG1*,<sup>4</sup> *MoATG4*,<sup>5</sup> *MoATG5*,<sup>6</sup> *MoATG8*,<sup>7,8</sup> *MoATG9*,<sup>9</sup> and *MoATG24*,<sup>10</sup> etc, has established the link between autophagy and fungal development. A systematic characterization of 16 genes essential for nonselective autophagy in *M. oryzae* demonstrates that autophagy is important for the establishment of rice blast disease.<sup>11</sup> Overall these studies demonstrate a critical role of autophagy, including nonselective autophagy and some selective types of autophagy (e.g. mitophagy), in *M. oryzae* conidiation and/or infection. Autophagy likely serves diverse functions including programmed cell death, maintaining integrity of lipid bodies, and glycogen catabolism.<sup>4,7,8</sup>

Autophagy is a highly conserved catabolic process in eukaryotes, responsible for vacuolar (lysosomal) degradation of proteins, membranes and organelles. Autophagy is induced during several biological processes in response to environmental stress or pathogen invasion, and cellular remodeling during development and differentiation.<sup>12–14</sup> The molecular basis of autophagy has been thoroughly investigated in yeasts and mammalian cells, by identification and functional characterization of 41 ATG genes (AuTophagy) thus far.<sup>15–17</sup> Among these genes, *ATG8* has been established as the most reliable marker for autophagy induction and autophagy-associated vesicular compartments.<sup>18–20</sup> *MoATG8*, the homolog of the yeast *ATG8*, is required for proper conidiation and pathogenicity in *M. oryzae*, and autophagy is naturally induced by light, the external stimulus for conidiation.<sup>8</sup> Light-induced autophagy can be visualized as vesicular RFP-Atg8 signal distributed in vegetative mycelia as well as conidiation-related structures, including aerial hyphae, conidiophore and conidia.<sup>8</sup> The findings pave the way to investigate the molecular mechanisms underlying such light-induced autophagy.

Recent studies unveil that histone acetyltransferase (HATs) and the histone deacetylases (HDACs) can directly modify autophagy proteins to regulate autophagy induction.<sup>21–23</sup> Our

**CONTACT** Yi Zhen Deng  [dengyz@scau.edu.cn](mailto:dengyz@scau.edu.cn)  Keji Building #402, South China Agricultural University, Guangzhou 510642, China.

<sup>†</sup>Co-first authors.

 Supplemental data for this article can be accessed on the [publisher's website](#).

© 2017 Shulin Zhang, Meiling Liang, Naweed I. Naqvi, Chaoxiang Lin, Wanqiang Qian, Lian-Hui Zhang, and Yi Zhen Deng. Published with license by Taylor & Francis. This is an Open Access article distributed under the terms of the Creative Commons Attribution-Non-Commercial License (<http://creativecommons.org/licenses/by-nc/3.0/>), which permits unrestricted non-commercial use, distribution, and reproduction in any medium, provided the original work is properly cited. The moral rights of the named author(s) have been asserted.

previous study on phototropism in *M. oryzae* identifies a HAT-encoding gene, *GCN5*, as light responsive.<sup>24</sup> HATs catalyze acetylation of histones on specific lysine residues,<sup>25</sup> and thus epigenetically regulate global gene transcription, stress response, and metabolic flux in plants<sup>26-28</sup> and yeasts.<sup>29,30</sup> The family of GNATs (*GCN5*-related N-acetyltransferases) also has a function in drug resistance in bacterial pathogens.<sup>31,32</sup> Recent clinical evidence suggests that Gcn5 may play a role in the pathology of cancer, asthma, COPD (chronic obstructive pulmonary disease) and Parkinson disease.<sup>33,34</sup>

In this study, we identified Gcn5 as an autophagy repressor in *M. oryzae*. The Gcn5 protein may shuttle between the cytosol and nucleus, and undergo post-translational cleavage and/or degradation in response to light. Our results suggest that Gcn5 acetylates Atg7 and thus represses autophagy in dark. Furthermore, Gcn5 may also regulate transcription of conidiation-related transcriptional regulator gene *TFB5*. Taken together, we propose that light induces *TFB5* transcription via Gcn5, and meanwhile derepresses autophagy by removing the Gcn5-catalyzed acetylation on Atg7, to promote asexual reproduction in the rice blast fungus.

## Results

### Identification of the *GCN5* genes in *M. oryzae*

We found 2 *GCN5* genes, *MGG\_03677* and *MGG\_11716* in the *M. oryzae* genome. Sequence identity and similarity between

these 2 Gcn5 proteins was 69.7% and 78.9%, respectively, as predicted by Needle ([http://www.ebi.ac.uk/Tools/psa/emboss\\_needle/](http://www.ebi.ac.uk/Tools/psa/emboss_needle/); Fig. S1). We named *MGG\_03677* as *GCN5*, and *MGG\_11716* as *GCN5b*. Given that our previous study on phototropism in *M. oryzae* identifies *MGG\_03677* as a light-inducible gene<sup>24</sup> while *MGG\_11716* does not seem to respond to light exposure at the transcriptional level (data not shown), we focused here on *GCN5* (*MGG\_03677*) as a candidate gene to investigate phototropic induction of autophagy and conidiation in *M. oryzae*.

### *Gcn5* negatively regulates autophagy

To investigate the relationship between Gcn5 (which hereafter refers exclusively to *MGG\_03677*) and autophagy during light-induced conidiation, we generated the *gcn5* $\Delta$  mutant by homologous recombination (Fig. S2A), and the *GCN5OX* strain (that overexpresses an N-terminal tagged GFP-Gcn5 fusion protein), both in an *RFP-ATG8* background. The *gcn5* $\Delta$  mutant, and the *GCN5OX* strain were verified by Southern blot (Fig. S2B), and the transcriptional level of *GCN5* in the *gcn5* $\Delta$  mutant or *GCN5OX* strain was examined by RT-PCR, with the wild-type (WT) *RFP-ATG8* strain as control (Fig. S2C).

Next, we examined phototropic induction of autophagy in the *gcn5* $\Delta$  and *GCN5OX* strains. Autophagy was induced by light in the WT strain, visualized as punctate or vacuolar RFP-Atg8 signals (Fig. 1A), whereas in the *gcn5* $\Delta$  mutant, RFP-Atg8

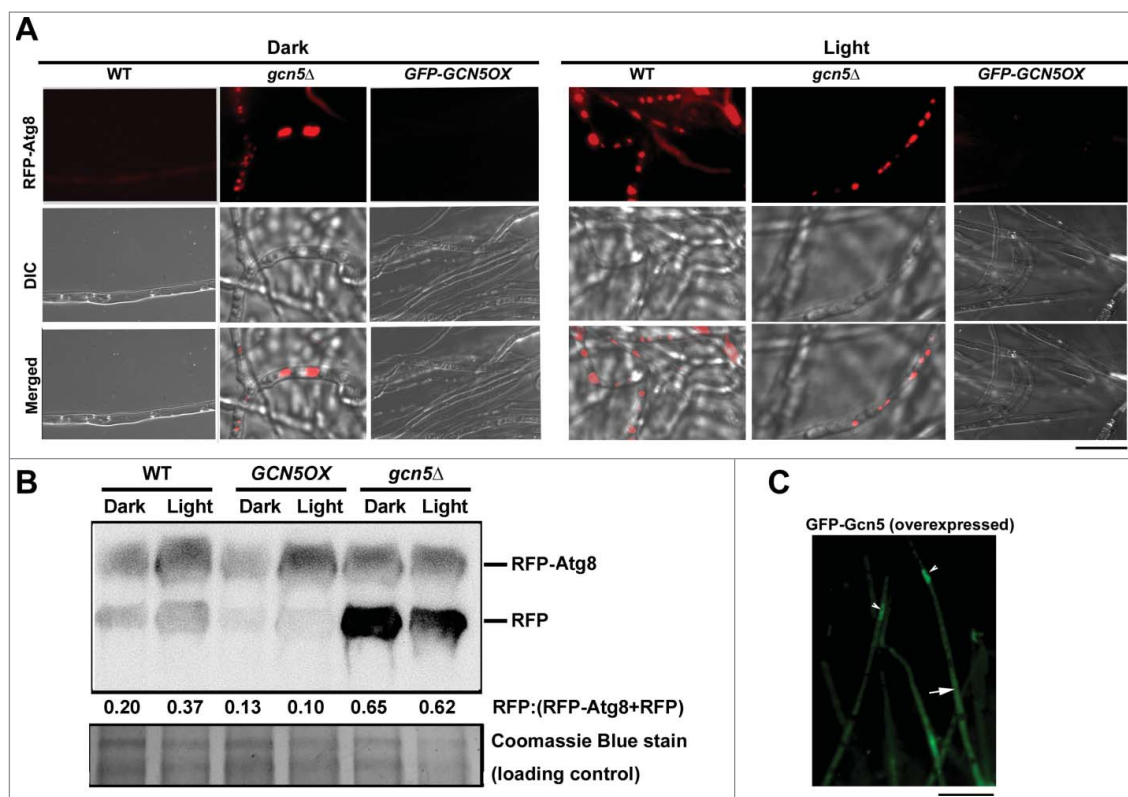


**Figure 1.** Gcn5 represses light-induced autophagy. (A) RFP-Atg8 in dark- or light- cultured mycelia of the WT, *gcn5* $\Delta$  and *GCN5OX* strains. Scale bar: 5  $\mu$ m. (B) Total protein lysates from the indicated strains were analyzed by immunoblotting with anti-RFP antibodies, under light or dark conditions. The extent of autophagy was estimated by calculating the amount of free RFP compared with the total amount of intact RFP-Atg8 and free RFP (the numbers appear underneath the blot). Densitometric analysis was performed using ImageJ (<https://imagej.nih.gov/ij/>). (C) GFP-Gcn5 signal in the *GCN5OX* strain appears nuclear (arrowhead) as well as cytosolic (arrow). Scale bar: 5  $\mu$ m. DIC, differential interference contrast.

appeared as small vesicles (autophagosomes) or vacuoles in both dark or light culture conditions (Fig. 1A). In contrast, RFP-Atg8 was undetectable in the *GCN5OX* mycelia grown either in presence or absence of light (Fig. 1A). The immunoblot analysis supported our interpretation that Gcn5 represses autophagy in *M. oryzae*. In WT, the amount of RFP peptide (cleaved from RFP-Atg8 fusion protein when autophagosomes fused with vacuoles; the band at the size of 26 kDa) was elevated/induced in response to light (Fig. 1B), suggesting that autophagy induction was enhanced. In the *GCN5OX* strain, however, little or no RFP band was detected in dark or light conditions (Fig. 1B). Autophagy activity was elevated upon loss of Gcn5, as RFP was detected in both dark and light conditions in the *gcn5Δ* mutant (Fig. 1B). Overall, we conclude that light-induced autophagy is repressed by Gcn5, although *GCN5* was initially identified as a light-inducible gene in *M. oryzae*.

We examined the subcellular localization of the Gcn5 protein in either light or dark conditions, by visualizing the overexpressed GFP-Gcn5 signal. GFP-Gcn5 appeared cytosolic (Fig. 1C, arrow) as well as nuclear (Fig. 1C, arrowhead). We costained the *GFP-GCN5* mycelia with the fluorescent dye DAPI to verify the nuclear localization. Punctate GFP-Gcn5 colocalized well with the DAPI-stained nuclear compartment (Fig. S2D), thus confirming its nuclear localization. We infer that Gcn5, the histone modifier, likely moonlights as a cytosolic protein during asexual development in *M. oryzae*.

To test whether the repression on autophagy by Gcn5 is through transcriptional regulation of the *ATG8* gene, we performed RT-PCR using total RNA from the mycelial cultures of WT, *GCN5OX* and *gcn5Δ* mutant exposed to light for 0, 2, 4, and 6 h. The input of total RNA was normalized and served as loading control (Fig. S2E). *ATG8* transcripts at different time points of light exposure were in general comparable in the same strain (Fig. S2E), which seems to rule out the possibility that the light induced Gcn5 may regulate autophagy via repressing *ATG8* transcription. However, we noticed that *ATG8* transcripts were overall lower in the *gcn5Δ* mutant than that in the WT or the *GCN5OX* strain (Fig. S2E), indicating that Gcn5, the histone modifier and transcriptional activator, may at least partially play a role in activating *ATG8* transcription. Nevertheless, given that autophagy was hyperinduced, instead of reduced, in the *gcn5Δ* mutant, compared with that in the WT (Fig. 1A and B), and that Gcn5 might be partially required for transcriptional expression of *ATG8*, we conclude that repression of autophagy by Gcn5 does not occur via transcriptional modulation of *ATG8*.

Considering that starvation is a well-established external stimulus to induce autophagy,<sup>35</sup> although *M. oryzae* conidiation could not be induced solely by starvation in dark (our unpublished data), we next asked whether starvation-induced autophagy is repressed by Gcn5. The vegetative mycelia of WT, *gcn5Δ* and *GCN5OX* mutants were cultured in CM (nitrogen replete) and shifted to MM-N (nitrogen starvation) for further 6 h to induce autophagy. Interestingly, autophagy was induced in the *gcn5Δ* mutant even in CM, while induction of autophagy was repressed by overexpressed *GCN5*, under nitrogen starvation as shown by microscopic analysis (Fig. 2A). Under extended nitrogen starvation (12 h), RFP-Atg8 appeared as

faint punctate structures in the cytosol, and was undetectable in the vacuoles in the *GCN5OX* mutant (Fig. S2F). In contrast, WT mycelia showed spherical vacuoles, with weak RFP signal in its lumen (Fig. S2F, arrowheads) under such extended starvation. We inferred that prolonged nitrogen starvation in the presence of continuous light, results in an incomplete or aberrant induction of autophagy, as visualized by the RFP-Atg8 puncta that failed to fuse with the vacuoles. Such RFP-Atg8 puncta likely represent incomplete PAS (phagophore assembly site) structures. Biochemical analysis using CM (nitrogen-replete) cultured and nitrogen starved (12 h) mycelia of WT, *GCN5OX* and *gcn5Δ* strains confirmed that nitrogen starvation based autophagy induction was also repressed by overexpressed *GCN5* while hyperactivated with loss of the *GCN5* gene (Fig. 2B). Cumulatively, the above results demonstrate that Gcn5 also represses autophagy in *M. oryzae* under nitrogen starvation conditions.

### **Gcn5 represses autophagy by acetylation of Atg7**

We screened for potential regulator(s) of autophagy in response to light by immunoprecipitation using GFP-Gcn5 as bait (Fig. S2G), and identified the immunoprecipitated (IP) proteins by mass spectrometry. GFP and Gcn5 proteins were among the identified proteins thus further validating the reliability of our earlier results. As expected, histones 2B, 3 and 4 were all identified as the Gcn5-interacting proteins (data not shown), confirming the involvement of Gcn5 in acetylation of histones. More importantly, we identified several proteins with established functions in autophagy regulation, including autophagy proteins Atg8 and Atg27 (Table 1), which might also physically interact with Gcn5.

We further compared the acetylated proteins differentially present in *GCN5OX* and *gcn5Δ* mutants, and identified the possible acetylated lysine residue(s), by LC-MS/MS. Selected acetylated proteins and the predicted acetylated residues are listed in Table 2. As expected, histones 2A, 2B, 2A.Z, 3, 3-like and 4 were identified, indicating the reliability of the LC-MS/MS analyses. Noticeably, most of the acetylated lysine residues were present in both *GCN5OX* and *gcn5Δ* samples, and at comparable levels ( $0.5 < \text{intensity ratio} < 2$ , Table 2). This suggests that acetylation of histone proteins did not depend entirely on the Gcn5 function. Among the acetylated proteins identified, we noticed that Atg7, encoded by *MGG\_07297*, contained an acetylated lysine residue at 338, which was present only in the *GCN5OX* strain but absent in *gcn5Δ* (Fig. 3A; Table 2). This indicated that acetylation of Atg7 at K338 might be specifically catalyzed by Gcn5. Interestingly, another identified acetylated site, Lysine107, did not depend on Gcn5 function as it was acetylated in the *gcn5Δ* mutant as well as in the *GCN5OX* strain (Table 2).

Atg7 is a ubiquitin-like modifier-activating enzyme that participates in post-translational processing of Atg8 for autophagy induction.<sup>36</sup> Therefore, we speculated that acetylated Atg7 may be an inactive form and that light induces autophagy by removing such Atg7 acetylation. To test this hypothesis, we expressed an Atg7-RFP fusion protein in both the WT and *GCN5OX* backgrounds, and observed the subcellular localization of Atg7-RFP fusion protein in the dark-light

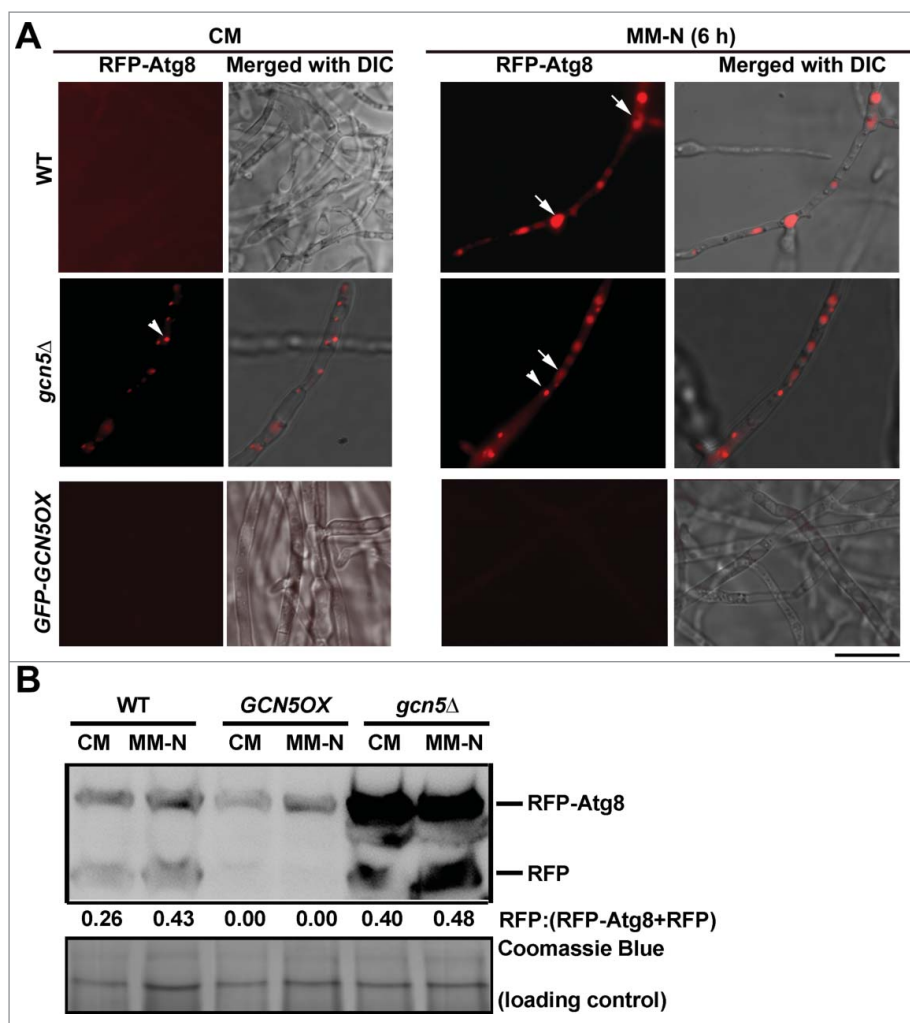


**Figure 2.** Gcn5 represses starvation-induced autophagy. (A) Gcn5 negatively regulates autophagy under nitrogen starvation conditions. RFP-Atg8 in CM- or MM-N-cultured mycelia of the WT, *gcn5Δ* and *GCN5OX* strains. Scale bar: 5  $\mu$ m. (B) Total protein lysates from WT, *gcn5Δ* and *GCN5OX* strain were analyzed by immunoblotting with anti-RFP antibodies. The extent of autophagy was estimated by calculating the amount of free RFP compared with the total amount of intact RFP-Atg8 and free RFP (the numbers appear underneath the blot). Densitometric analysis was performed using ImageJ (<https://imagej.nih.gov/ij/>).

**Table 1.** List of identified Gcn5-interacting proteins related to autophagy.

Gene ID/name	Uniprot ID	MW	Mascot score*	E-value
MGG_00446/CK2 subunit $\beta$ (beta)	L7IH74	38927.6	67.7	3.14E-06
MGG_03696/CK2 subunit $\alpha$ (alpha)	L7J0C6	39488.7	66.54	1.15E-05
MGG_05651/CK2 subunit $\beta$ (beta)-2	G4MNM6	31287.6	51.26	2.96E-05
MGG_06962/Ypt1	G4MNT9	70759.72	40.21	6.39E-03
MGG_06154/Ras-like protein	G4MZY8	24097.9	46.72	4.73E-02
MGG_07176/GTP-binding protein Rho1	L7I1M4	21830	54.13	1.64E-04
MGG_01607/Calnexin	L7IX88	63854.2	48.9	2.97E-04
MGG_06860/Coatomer subunit $\beta$ (beta)	L7J3Z0	106213	31.45	1.99E-02
MGG_14666/SEC13	L7JMJ6	31915.1	40.22	4.92E-03
MGG_06910/SEC23	A4R1J7	85917.3	31.25	5.29E-02
<b>MGG_01062/Atg8</b>	B6VCT7	14369.3	29.14	5.27E-02
MGG_09565/Pmk1	G4N0Z0	41303	27.08	6.40E-02
MGG_09499/Ras-2	G4N1S3	26891.3	30.03	2.54E-02
MGG_07145/Cullin-1	L7HTP0	88223.7	23.23	6.73E-02
MGG_09564/SEC24	L7I4V3	116723	20.02	1.38E-01
MGG_04830Vps26B	L7IJI1	35801.6	22.41	1.04E-01
<b>MGG_02386/Atg27</b>	L7IPM7	38353.7	49.08	2.56E-04
MGG_03511/Coatomer subunit $\alpha$ (alpha)	L7IXA5	136066	21.49	2.19E-01
MGG_09294/Coatomer subunit $\zeta$ (Zeta)	L7J2Q7	22247.3	20.92	3.72E-02
MGG_00345/Rim15 kinase	L7JKF9	212094	29.23	7.46E-03

\*Masct score  $\geq 20$  as threshold.

cycles. Atg7-RFP appeared cytosolic in dark-grown mycelia in the WT, whereas it became punctate, presumably corresponding to the PAS, or vacuolar in response to light exposure (Fig. 3B). In contrast, Atg7-RFP remained cytosolic in *GCN5OX* mycelia in both dark and light culture conditions (Fig. 3B, arrowheads). We further detected Atg7 acetylation by immunoblot with RFP-Trapped proteins against the anti-acetyl lysine (anti-acK) antibody. Acetylation of Atg7 appeared higher in the *GCN5OX* mutant, both in dark or light conditions, compared with the WT (Fig. 3C). The acetylation level of Atg7-RFP protein decreased significantly in response to light exposure in the WT, while it was retained in the *GCN5OX* strain, likely due to prolonged activity and function of Gcn5 therein (Fig. 3C). Similarly, overexpression of *GCN5* resulted in elevated levels of Atg7 acetylation even under nitrogen starvation (Fig. 3D). Nitrogen starvation also induced punctate Atg7-RFP in WT mycelia, whereas cytosolic Atg7-RFP was predominant in the *GCN5OX* mycelia cultured both in rich or nitrogen-depleted medium (Fig. 4A). These results indicate that starvation-induced autophagy could also be effectively repressed by continued Gcn5-catalyzed acetylation of Atg7.

**Table 2.** List of predicted acetylated proteins and sites.

Protein ID	Protein	Sequence window	Score	Modified sequence	Charge	m/z	Intensity OX/delt
<b>Histone proteins</b>							
>tr G5EHN4 G5EHN4_MAGO7	Histone H4	___MTGRGKGGKGLGKGGAKRHRKILRDNIQ	151.44	_GLGK(ac)GGAK(ac)R_	2	464.272	0.65
		TGRGKGGKGLGKGGAKRHRKILRDNIQGITK	151.44	_GLGK(ac)GGAK(ac)R_	2	464.272	0.65
		___MTGRGKGGKGLGKGGAKRHRKILR	90.696	_GK(ac)GGK(ac)GLGK_	2	443.261	0.78
>tr L7ICZ8 L7ICZ8_MAGOY	Histone H3	RKSTGGKAPRQLASKAARKSAPSTGGVKKP	185.6	_QLASK(ac)AAR_	2	443.759	0.55
		YKPGTVALREIRRYQKSTELLIRLRFQRLV	285.83	_YQK(ac)STELLIR_	2	646.864	0.26
		TKQTARKSTGGKAPRQLASKAARKSAPSTG	185.6	_K(ac)QLASK(ac)AAR_	2	528.812	0.53
		_MARTKQTARKSTGGKAPRQLASKAARKSA	138.08	_STGGK(ac)APR_	2	408.222	1.18
		___MARTKQTARKSTGGKAPRQLASKA	138.08	_K(ac)STGGK(ac)APR_	2	493.275	0.77
>tr G4N793 G4N793_MAGO7	H3-like centromeric protein cse-4	YRPGTLALREIRRYQKSTDLLMRKLPFARLV	110.66	_RYQK(ac)STDLLMR_	3	484.926	0.00
>sp L711W3 H2B_MAGOY	Histone H2B	___MPPKAADKPKASKAPATASKAPEKKDAG	168.98	_PASK(ac)APATASK(ac)APEK_	2	769.415	1.03
		___MPPKAADKPKASKAPATASKAPE	127.76	_AADK(ac)K(ac)PASK_	2	500.277	1.22
		APATASKAPEKKDAGKTAASGDGKKRTR	135.02	_DAGK(ac)K(ac)TAASGDG_	2	616.81	1.32
		___MPPKAADKPKASKAPATASKAPE	127.76	_AADK(ac)K(ac)PASK_	2	500.277	1.22
>sp L7HZV6 H2A_MAGOY	Histone H2A	___MTGGGKSSGGKASGSKNAQSR	113.4	_(ac)TGGGK(ac)SSGGK(ac)ASGSK_	2	652.826	0.74
		GGKASGSKNAQSRSSKAGLAFVGRVHLLR	58.674	_SSK(ac)AGLAFVGR_	2	616.343	0.00
		___MAGGKSSGGKSSGGKTSSEGPKKQ	121.28	_SSGGK(ac)SSGGK(ac)TSSEGPK_	2	796.382	0.81
		AGGKSSGGKSSGGKTSSEGPKKQSHSAR	80.638	_SSGGK(ac)SSGGK(ac)TSSEGPK_	2	796.382	1.05
>sp A4QVR2 H2AZ_MAGO7	Histone H2A.Z	___MAGGKSSGGKSSGGKTSSEGPKKQ	121.28	_GK(ac)SSGGK(ac)SSGGK_	2	560.783	0.49
<b>Autophagy Proteins</b>							
>tr L7HTU6 L7HTU6_MAGOY	Ubiquitin-like modifier-activating enzyme ATG7	SEMPKVTGWERHPSSKQARVISLAEYMDPT	66.299	_HPSSK(ac)LQAR_	2	533.294	∞
		RADGSIRNFNTIEDFKADKAILRQAGAQI	881.865	_NFNTIEDFK(ac)K_	2	649.325	0.35

### Light-dependent transcriptional regulation of GCN5

It was puzzling that light-inducible *GCN5* could repress the photo-induced autophagy in *M. oryzae*. To explore possible light-dependent regulation of Gcn5 function, we attempted to screen for light responsive elements (LREs) in the promoter region of *GCN5*. Two Gap boxes as 5'-ATGAA(G/A)A-3' repeats essential for light induction of the *GapA* and *GapB* genes in plants<sup>37</sup> were found at -936 to -928 and -918 to -911 (Fig. 4B, green highlighted). In addition, a 5'-CACGTG-3' E-box sequence, which is a negative regulatory element modulating light-dependent gene expression identified in flies,<sup>38</sup> was also found at -179 to -173 (Fig. 4B, red highlighted). We generated the constructs carrying *eGFP* reporter gene under the control of WT, M1 or M2 mutated promoters of *GCN5*, as illustrated in Fig. 4B, and individually expressed them in the wild-type *M. oryzae* strain. The light-dependent regulation of *GCN5* promoter activity was verified by RT-PCR with *eGFP*-specific primers (Fig. 4C, Table S1). In parallel, we tested the transcription of *GCN5* during the time-course analysis of light exposure, using RT-PCR with *GCN5*-specific primers (Table S1), and found that the *GCN5* transcripts were increased substantially during the time-course of light exposure (Fig. 5C).

Under an epifluorescence microscope, WT-eGFP showed faint/weak signal in dark and was significantly enhanced under light (Fig. S3A). M1-eGFP showed a relatively higher eGFP signal in both dark and light conditions, compared with that in WT-eGFP (Fig. S3A), confirming that E-box serves as a negative element to repress gene expression in the dark. On the other hand, M2-eGFP was not induced by light (Fig. S3A), suggesting the key role of Gap boxes in light

signaling. The light-dependent regulation of *GCN5* promoter activity was further verified by immunoblot with anti-GFP antiserum (Fig. S3B).

Overall, we conclude that the Gap box acts as a positive element for light-induced expression of *GCN5*, while the E-box represses the *GCN5* transcription in the dark and confers the light-dependent expression of *GCN5* together with the Gap box.

### Post-translational processing of Gcn5 in response to light

We generated a strain with *GCN5-mCherry* driven by its native promoter and at its genomic locus, as illustrated in Figure S3C. In the dark, Gcn5-mCherry signal was undetectable or appeared as dim, cytosolic signal (Fig. 4D). At 12h post-photo-induction, we observed weak nuclear localization of Gcn5-mCherry, which overlapped with Tfb5-GFP, a nuclear marker specific to light induction (Fig. 4D and S3D).<sup>24</sup> In immunoblot analysis using anti-RFP antibody, 2 bands of approximately 36 and 20 kDa were detected, and were clearly more abundant in light-cultured mycelia (Fig. S3E, denoted by #). We infer that these were partial Gcn5-mCherry fusion protein variants, as the size was smaller than the calculated molecular mass of full-length Gcn5-mCherry (Gcn5 as approximately 44 kDa and mCherry as 26 kDa, Fig. S3C). The cleaved C-terminal region of Gcn5 tagged with mCherry was calculated as 9 to 10 kDa, corresponding to about 100 amino acids. As shown in the schematic representation of Gcn5 protein domain organization (Fig. S3C), Gcn5 contains an N-terminal acetyltransferase (NAT) domain that catalyzes histone

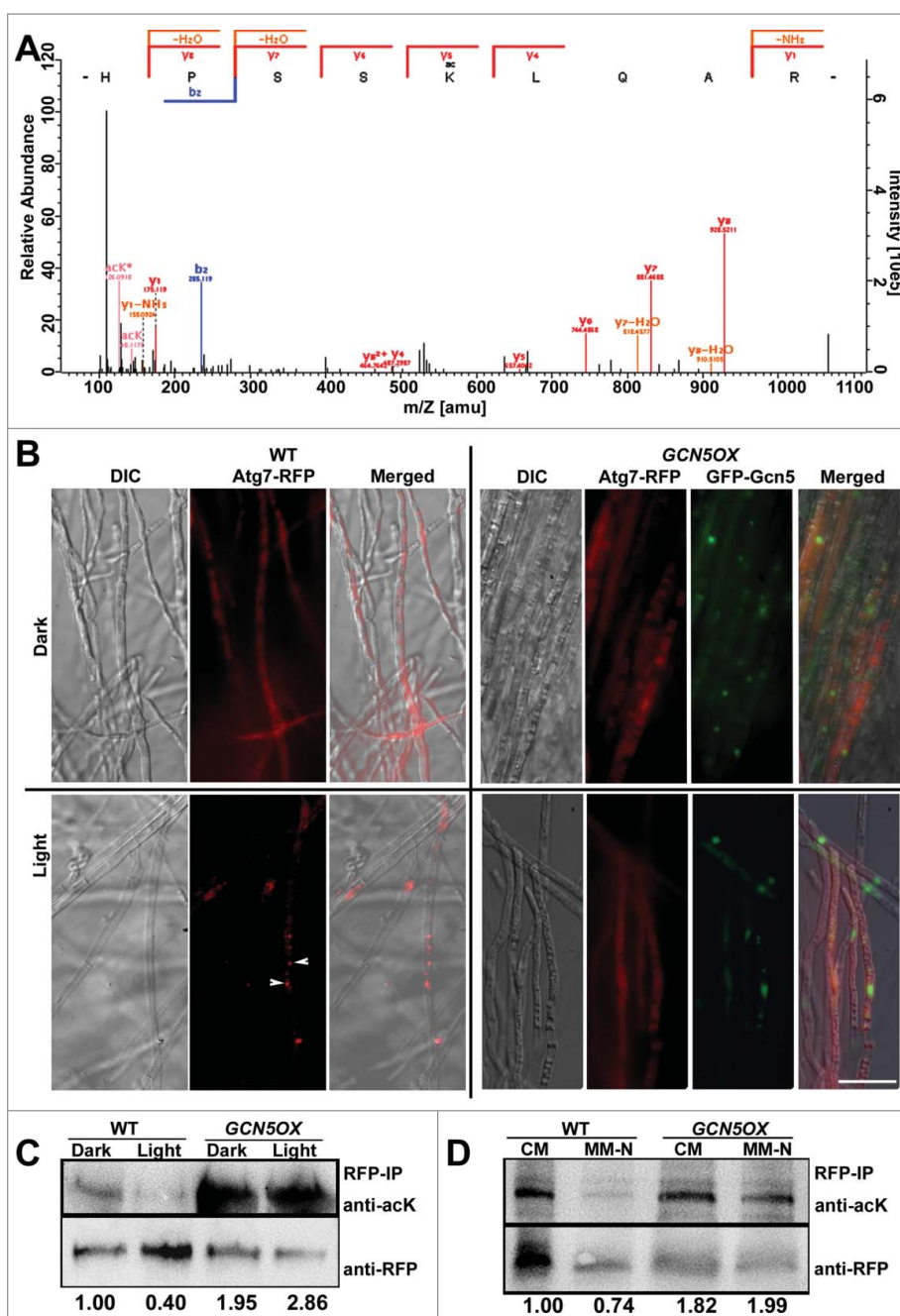


**Figure 3.** Gcn5 represses autophagy via acetylation on Atg7. (A) Identification of Atg7 K338 acetylation by means of liquid chromatography–mass spectrometry (LC-MS)/MS analysis. The MS/MS spectrum of a double-charged ion at mass/charge ratio ( $m/z$ ) 533.294 for  $MH_2^{2+}$  corresponding to the mass of the acetylated peptide HPSSK(ac)LQAR. The labeled peaks correspond to masses of  $b$ ,  $y$  ions of acetylated peptide fragments. (B) Subcellular localization of Atg7-RFP in WT and *GCN5OX* mycelia cultured in dark-light cycle. Arrowhead depicts punctate Atg7-RFP signal in WT mycelia exposed to light for 6 h. Arrow, vacuole. Scale bar: 10  $\mu$ m. (C) RFP-IP (immunoprecipitated) proteins from total lysates of dark or light cultured WT or *GCN5OX* mutant were subjected to immunoblotting with anti-acK antibody. Detection with anti-RFP serves as loading control. Relative abundance of acetylated Atg7 was calculated as a ratio of acK/RFP band, with densitometric analysis performed by ImageJ software (<https://imagej.nih.gov/ij/>). The numbers under the blots are relative fold change, as normalized to the lane of WT dark, which was arbitrarily set as 1.00. (D) RFP-IP (immunoprecipitated) proteins from total lysates of liquid-cultured WT or *GCN5OX* mutant, in either rich (CM) or nitrogen-depleted (MM-N) medium, were subjected to immunoblotting with anti-RFP antibody. Detection with anti-RFP serves as loading control. The relative fold changes of acetylated Atg7 were calculated following the same way as in Figure 3C, and labeled under the blots.

acetylation, and a C-terminal bromodomain, that interacts specifically with acetylated lysine. The cleaved C-terminal 100-amino acid peptide of Gcn5 corresponds exactly to the bromodomain. We inferred that histone acetylation increases in response to light exposure, leading to increased association between acetylated histone and Gcn5 bromodomain, resulting in its nuclear retention. The subcellular localization of the NAT domain was not visualized by

Gcn5-mCherry, but could be followed in the *GFP-GCN5OX* strain, as both nuclear and cytosolic (Fig. 1C). Immunoblot with anti-GFP antibody against total lysates from dark- and light-cultured *GFP-GCN5OX* strain confirmed that a cleavage occurs between the NAT domain and the C-terminal bromodomain, as a band corresponding to 60 kDa was detected (Fig. S3F, triangle) and assumed as GFP-NAT. The full-length GFP-Gcn5 fusion protein (70 kDa) was also

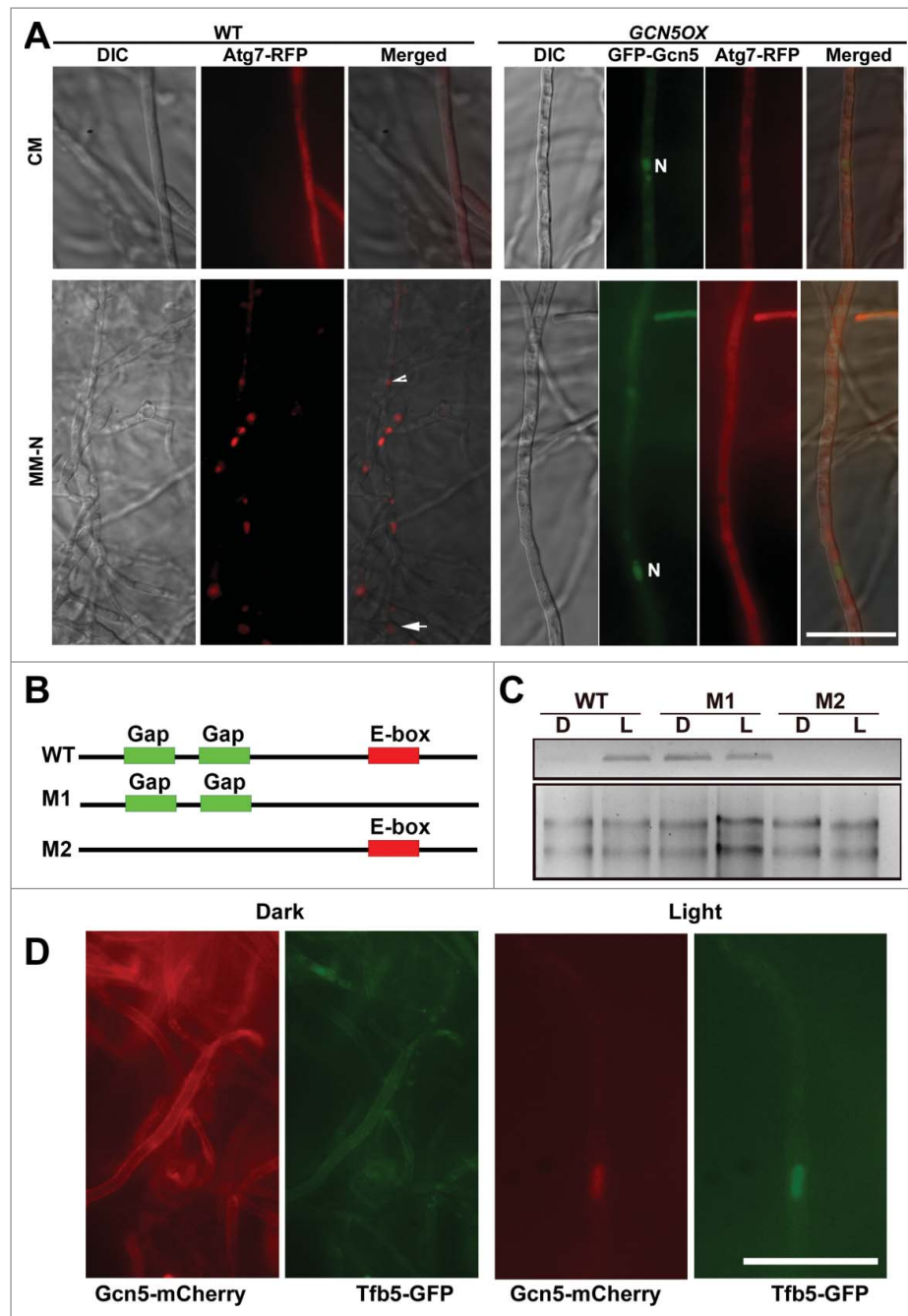


**Figure 4.** Transcriptional and post-translational regulation of Gcn5 during dark-light cycles. (A) Subcellular localization of Atg7-RFP in WT and *GCN5OX* mycelia cultured in rich (CM) medium or under nitrogen starvation for 6 h. Scale bar: 10  $\mu\text{m}$ . "N" denotes nuclei visualized by GFP-Gcn5; arrow and arrowhead depict vacuolar and punctate Atg7-RFP signal, respectively. (B) Schematic representation of the *GCN5* promoter, not drawn to scale. Green boxes represent Gap boxes and red box as E-box. (C) *GFP* transcription driven by WT, M1 or M2 variant of the *GCN5* promoter was examined by RT-PCR. Primers used for RT-PCR are listed in Table S1. Total RNA (2  $\mu\text{g}$ ) serves as a loading control. (D) Subcellular localization of Gcn5-mCherry under dark or light conditions. Arrow denotes the colocalization of Gcn5-mCherry with nuclear Tfb5-GFP, upon light induction. Scale bar: 10  $\mu\text{m}$ .

detected (Fig. S3F, asterisk), and it appeared more abundant in the dark-cultured mycelia than in the light-cultured mycelia, likely due to light-triggered cleavage of Gcn5. The cleaved NAT domain may be unstable, as multiple bands of various sizes were detected, likely as intermediates of protein degradation (Fig. S3F, double triangles). A 26-kDa fragment, corresponding to GFP peptide alone, was also detected (Fig. S3F, double asterisk). Overall, we propose that the NAT domain and the bromodomain of Gcn5 protein are likely cleaved and separated upon light induction.

The bromodomain was retained in the nucleus, likely by associating with the acetylated histones; while the cytosolic NAT domain was subjected to subsequent degradation. This could partially explain why light-inducible *GCN5* represses light-induction of autophagy in *M. oryzae*: as light likely destabilizes the Gcn5 protein and thus relieves its repression on autophagy via Atg7 acetylation. In the dark, although the *GCN5* transcription is low, the basal level of Gcn5 protein may be intact and stable, and it localizes in the cytosol to keep Atg7 acetylated and inactive.

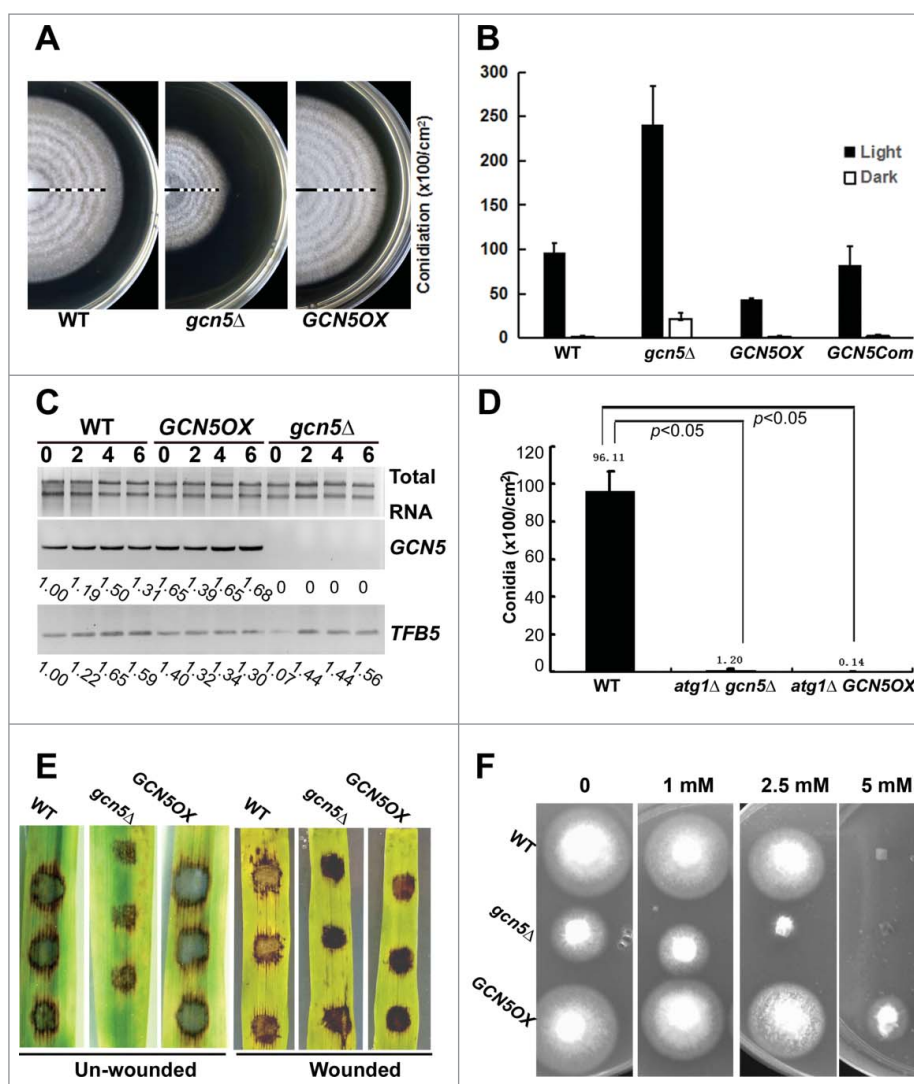


**Figure 5.** Biological functions of Gcn5. (A) Banding pattern of the WT, *gcn5Δ* and *GCN5OX* strains. Closed bar represents the growth phase in dark, and open bar for growth under light. Five dark-light (12 h-12 h) cycles were given following growth in constant dark for 3 d. The PA medium supporting mycelial growth was kept at 60°C for 3 to 5 h, for fast dehydration to achieve better contrast of the banding, before photography. (B) Bar chart depicting quantitatively assessed conidiation in the indicated strains, grown in dark or light conditions. Mean values ( $\pm$  SE) presented as percentage points were derived from 3 independent experiments ( $n = 15$  colonies for each sample). (C) *TFB5* transcripts in WT, *gcn5Δ* and *GCN5OX* cultures exposed to light for 0, 2, 4 and 6 h. Total RNA (2  $\mu$ g) serves as a loading control. Primers used for RT-PCR are listed in Table S1. (D) Bar chart depicting quantitatively assessed conidiation in the indicated strains. Mean values ( $\pm$  SE) presented as percentage points were derived from 3 independent experiments ( $n = 15$  colonies for each sample). (E) Barley leaf explants (intact or wounded) were inoculated with conidia from the indicated strains and disease symptoms assessed after 7 d. (F) Sensitivity toward oxidative stress was tested in the WT, *gcn5Δ* and *GCN5OX* strains, cultured on PA solid medium supplemented with H<sub>2</sub>O<sub>2</sub> at concentration of 0 (control), 1, 2.5, 5, and 10 mM.

### Gcn5 regulates *M. oryzae* conidiation

We further investigated the biological function of Gcn5 by analyzing vegetative growth, circadian banding of vegetative colony in dark-light cycles, conidiation and pathogenicity of the *gcn5Δ*, *GCN5*-complemented strain and *GCN5OX* mutants, with WT strain as a control. Radial growth was significantly slower in the *gcn5Δ* mutant (radius =  $1.53 \pm 0.02$  cm;  $P < 0.01$ ), while marginally faster in the *GCN5OX* mutant (radius =  $2.35 \pm 0.03$  cm;  $0.05 < P < 0.1$ ), compared with WT (radius =  $2.28 \pm 0.02$  cm), after growth in dark for 7 d. The reduction of radial growth could be fully restored in the *GCN5*-complemented strain (radius =  $2.20 \pm 0.04$  cm;  $P = 0.18$ ), verifying that such growth defect was indeed caused by the loss of *GCN5* function. The banding of *gcn5Δ* colony was comparable to that of WT, although the mutant colony was smaller than

WT (Fig. 5A). Similarly, the *GCN5OX* strain showed a banding pattern comparable to that of WT (Fig. 5A), suggesting that Gcn5 may not be a core component or regulator of the circadian clock in *M. oryzae*.

Under the light, conidiation was largely increased in the *gcn5Δ* mutant, while reduced approximately 50% in the *GCN5OX* strain, compared with the WT (Fig. 5B,  $P < 0.05$ ). In the dark, the WT and the *GCN5OX* mutant produced hardly any conidia while the *gcn5Δ* mutant was able to produce significantly more conidia than the WT (Fig. 5B,  $P < 0.05$ ). The conidiation of the *GCN5*-complemented strain was comparable to that of the wild-type strain ( $P > 0.1$ ), but distinct from either the *gcn5Δ* mutant or the *GCN5OX* mutant ( $P < 0.05$ ; Fig. 5B). We previously showed that Tfb5 is a light-inducible transcriptional factor and essential for *M. oryzae* conidiation.<sup>23</sup> Here, we further verified whether overexpressed *GCN5* could repress



conidiation via transcriptional repression of the *TFB5* gene. As shown in Fig. 5C, *TFB5* was induced during the time-course of light exposure in the WT strain as well as in the *gcn5Δ* mutant, while it was constantly induced in the *GCN5OX* strain in either dark or light conditions (Fig. 5C). Therefore, we conclude that *GCN5* is involved but not essential for *TFB5* transcription, and the reduced conidiation in the *GCN5OX* strain is not caused by repression of the *TFB5* transcription.

We inferred that Gcn5 may repress conidiation in the dark, likely by repressing autophagy. To further confirm this hypothesis, we deleted the *ATG1* gene in both *gcn5Δ* and *GCN5OX* mutants (Fig. S4A and B), as *ATG1* has been reported to be essential for autophagy in *M. oryzae* as the *Moatg1Δ* mutant showed significant reduction in conidia production.<sup>4</sup> The resultant *atg1Δ gcn5Δ* double mutant was significantly reduced in conidiation (Fig. 5D,  $P < 0.05$ ), which was similar to the reported phenotypic defects of the *Moatg1Δ* mutant.<sup>4</sup> Conidiation was also reduced in the *atg1Δ GCN5OX* mutant (Fig. 5D,  $P < 0.05$ ). This suggests that conidiation phenotype observed in *gcn5Δ* and *GCN5OX* mutants were indeed related to autophagy activity.

Although the *gcn5Δ* mutant produced abundant conidia, such conidia were unable to infect the host successfully. Infection assays with barley leaf explants showed that the *gcn5Δ* conidia were significantly reduced in pathogenicity, while WT or *GCN5OX* conidia were able to cause typical blast disease lesions (Fig. 5E). The *gcn5Δ* conidia could better infect the wounded leaves than the intact leaves, however, the infection was still weaker than the wild-type conidia did, under the same conditions (Fig. 5E). Furthermore, regulation of autophagy as well as pathogenicity by the *GCN5* gene was verified (Fig. S4C and D).

The reduced pathogenicity upon *GCN5* deletion may result from the oxidative stress response mediated by Gcn5 as reported for its yeast, fungal or mammalian orthologs.<sup>30,39,40</sup> The sensitivity assay toward hydrogen peroxide further confirmed that *gcn5Δ* was hypersensitive to oxidative stress, compared with the WT or the *GCN5OX* strain (Fig. 5F). Pathogenicity assays with mycelial plugs of the *atg1Δ*, *atg1Δ gcn5Δ*, or *atg1Δ GCN5OX* strains were also performed, with intact or wounded barley leaves, and the result showed that these 3 strains were incapable of causing blast disease (Fig. S4E), consistent with the previous reports on the essential role of autophagy in *M. oryzae* infection.<sup>4,7</sup>

## Discussion

In eukaryotic organisms, HAT complexes are coactivators important for transcriptional activation by modifying chromatin.<sup>41-43</sup> In this study, we identified an ortholog of *GCN5* from *M. oryzae*, encoding a component of the HAT complex important for *M. oryzae* conidiation and pathogenicity. We also identified a *GCN5* paralog, namely *GCN5b*, in *M. oryzae* genome. *GCN5b* is not required for *M. oryzae* conidiation or pathogenicity and hence was not characterized further in this study. Recently, it has been reported that Hat1 regulates the stress response and virulence in *Candida albicans*.<sup>44</sup> The *GCN5* ortholog is involved in morphological transition and virulence in *C. albicans*<sup>45</sup> and *Ustilago maydis*.<sup>46</sup> But overall, the

knowledge on physiological functions of HAT or HDAC components and associated regulatory mechanisms in pathogenic fungi is really limited, and potential phototropic regulation of these Gcn5 HATs was not predicted or verified. To our knowledge, involvement of HAT in fungal asexual production has not been documented previously, therefore, the findings from this study add not only a new member to the list of HATs that are essential for fungal development and pathogenicity, but also further expand the biological functions modulated by HATs, and importantly, for the first time, reports a phototropic signaling pathway and a regulatory mechanism mediated by protein acetylation and deacetylation cycles.

A yeast HAT Esa1 and its mammalian ortholog KAT5/TIP60 acetylate Atg3/ATG3 or Atg1/(mammalian ULK1/2) respectively, to induce autophagy in response to physiological cues.<sup>21,22</sup> In *M. oryzae*, the Esa1 ortholog is not involved in regulating autophagy or conidiation (our unpublished data). Instead, Gcn5 represses autophagy, in contrast to yeast Esa1 or mammalian KAT5, without light. We found that Gcn5 directly acetylates Atg7 to repress autophagy induction, which is consistent with the observation that acetylation of ATG7 by EP300/p300 acetyltransferase in mammalian cells inhibits autophagy,<sup>47,48</sup> and that SIRT1-catalyzed deacetylation of autophagy protein is required for autophagy induction in mouse.<sup>49</sup> A recent study shows that anacardic acid, a nonspecific HAT inhibitor, is effective in preventing *M. oryzae* pathogenicity.<sup>50</sup> Anacardic acid has been demonstrated to directly inhibit histone acetyltransferases (HATs) like EP300/p300, KAT2B/PCAF and KAT5/Tip60<sup>51</sup> and to induce autophagy in human lung carcinoma A549 cells.<sup>52</sup> Our results are consistent with these reports in that the *gcn5Δ* mutant was reduced in pathogenicity, and showed elevated autophagy activity. Besides direct modification on cytosolic autophagy proteins, HATs including Gcn5 may also regulate autophagy via histone modification. It has been reported that histone H3 hyperacetylation in *Drosophila melanogaster*, is associated with transcriptional downregulation of several autophagy-essential *ATG* genes, including *ATG5*, *ATG7*, and *ATG14*, which may restrict autophagic activities.<sup>53</sup> Our study also proved that *ATG8* transcription was not repressed upon *GCN5* overexpression, instead, it depended on *GCN5* for its transcription (Fig. S2E). However, we did not rule out the possibility that overexpressed *GCN5* may also lead to hyperacetylation of target histones and likely downregulation of *ATG* genes, thus resulting in the observed repression of autophagy pathway.

Our results showed that Gcn5 is subject to regulation by a dark-light cycle via the positive and negative LREs located in its promoter region. Interestingly, we also found same LREs in *GCN5* orthologs in *C. albicans* and *Ustilago maydis*, as well as in the *Ep300/p300* acetyltransferase gene in *Mus musculus* (Fig. S4F), although whether these *GCN5* orthologs were also subjected to light modulation through LREs, remains to be functionally verified. Overall, our study demonstrates a novel light-responsive pathway mediated by Gcn5 to induce autophagy and conidiation in the rice-blast fungus *M. oryzae*. Such phototropic regulation on autophagy induction might be conserved in eukaryotic organisms, given that the LREs are conserved in the promoter regions of several HAT-encoding genes in other organisms. We are still unclear about the biological

significance of light-induction of *GCN5* transcription, as light subsequently destabilizes this gene product. We attempted to examine the dependence of conidiation-related gene *TFB5* transcription on *GCN5*, as yeast Gcn5 is known to be a *TFB5* activator,<sup>54</sup> in response to carbon homeostasis and/or hypoxia,<sup>55,56</sup> but not to light. Our result showed that *TFB5* transcripts accumulated in the WT strain during light exposure (Fig. 5C). Such light-induction of *TFB5* transcription was not dependent on *GCN5* as the level of *TFB5* transcription in the *gcn5Δ* mutant was comparable to that of WT (Fig. 5C). *TFB5* transcription was induced in the dark in the *GCN5OX* strain but showed no obvious increase in the light condition (Fig. 5C). This result indicates that Gcn5 is involved but not critical for *TFB5* activation, and the reduced conidiation in the *GCN5OX* strain was not caused by *TFB5* repression. We further infer that transcriptional induction of *GCN5* by light may be transient, to activate conidiation-related genes including *TFB5*.

In summary, we propose that light regulates *GCN5* expression, as well as stability and subcellular localization of Gcn5 protein during the dark-light cycles. Gcn5 represses autophagy via acetylation on Atg7 in the dark; while it releases repression of autophagy upon photo-induction and subsequent translocation into the nucleus and/or upon degradation. Phototropic induction of *GCN5* may contribute to transcriptional regulation of *TFB5*, which encodes a conidiation-specific transcription factor in *M. oryzae*. Such phototropic regulation of *GCN5* transcription and the stability of the subcellular localization of the Gcn5 protein promote robust light-induced autophagy as well as conidiation in *M. oryzae*. Future studies should certainly aim to identify the other targets of the Gcn5 transcriptional activator module, and further investigate the regulatory mode of *GCN5* function in *M. oryzae*.

## Materials and methods

### Fungal strains and growth conditions

The *M. oryzae* wild-type strain B157 (Field isolate, *mat1-2*) was originally obtained from the Directorate of Rice Research, India. *M. oryzae* strains were propagated on Prune-agar (PA) medium or complete medium (CM) as described.<sup>57</sup> The composition of MM-N (used for nitrogen starvation) was as reported previously.<sup>58</sup> To assess the growth and colony characteristics, *M. oryzae* isolates were cultivated on CM agar or PA medium, at 28°C for 1 wk. Mycelia used for total protein extraction were obtained by growing the relevant strains in liquid CM for 2 to 3 d, with gentle shaking, followed by inoculation in CM or MM-N for about 6 h. For quantitative analysis of conidiation and testing the pathogenicity, standard procedures were followed.<sup>59</sup>

### Plasmid constructs and fungal transformants

To generate *gcn5Δ*, the 5' UTR and 3' UTR were amplified and ligated sequentially into the *Agrobacterium* Transfer-DNA vector pFGL820 to flank the *ILV1* cassette.<sup>23</sup> The resultant plasmid was then transferred into the *M. oryzae* strain carrying an ectopic *RFP-ATG8*,<sup>8</sup> to induce a locus-specific knockout. To construct overexpressed *GFP-GCN5*, GFP was fused in frame

to the N-terminus of the *GCN5* ORF, and under the constitutive promoter of *RP27*.<sup>23</sup> The transformed *M. oryzae* was selected by bialaphos resistance, and with ectopic *GFP-GCN5*. To construct Gcn5-mCherry, mCherry was fused in frame to the last 0.5 kb of the *GCN5* ORF and the plasmid transformed into *M. oryzae*, such that the mCherry was fused to the *GCN5* coding sequence at its genomics locus. For *GCN5* complementation, the *GCN5* locus, including promoter region (1 Kb), ORF and terminator (0.3 Kb), was PCR-amplified and ligated into pFGL821 (addgene, 58223) WT, M1 and M2 varieties of the *GCN5* promoter were synthesized by Thermo-Fisher (Shanghai) and fused with the *eGFP* coding sequence respectively, on the vector pFGL932<sup>24</sup> (for M1 *GCN5Prom-eGFP*) or pFGL821 (for WT *GCN5Prom-eGFP* and M2 *GCN5Prom-eGFP*). To generate *atg1Δ*, the 5' UTR and 3' UTR were amplified and ligated sequentially into the vector pFGL821 to flank the *HPH1* cassette. The resultant plasmid was then transferred into the WT, *gcn5Δ* or *GCN5OX* strains, respectively, to induce a locus-specific knockout. For C-terminal tagging of Atg7 with dsRed, *ATG7* ORF was PCR amplified and ligated into pFGL932, under the *RP27* promoter. The fragment containing *RP27* promoter-*ATG7* was released by *Bam*HI/*Eco*RI double digestion and ligated to pFGL821, followed by ligation of PCR-amplified *dsRed* CDS into *Eco*RI site. The *RP27* Promoter-*ATG7-dsRed* sequence was introduced into the WT and *GCN5OX* strains, as an ectopic copy. The primers used for gene deletion, complementation and GFP, mCherry or dsRed tagging are listed in Table 3.

### Epifluorescence microscopy

*M. oryzae* cells expressing fluorescent protein-fused chimera were grown under requisite conditions. Epifluorescence microscopy was performed using an Axio Observer Z1 microscope (Zeiss, Jena, Germany) equipped with an sCMOS camera (PCO Edge, Kelheim, Germany). To visualize the nucleus, mycelia were fixed with 0.1% TritonX and stained with 1 μg/ml DAPI (Sigma-Aldrich, D9542) at room temperature for 10 min, followed by 3 washes with PBS.

### Immunoblotting and immunoprecipitation

For total protein extraction, mycelia grown under requisite conditions were ground into a fine powder in liquid nitrogen and resuspended in 0.3 to 0.5 ml extraction buffer (10 mM Tris-HCl, pH 7.5, 150 mM NaCl, 0.5 mM EDTA, 0.5% NONIDET P-40 Substitute (Sigma-Aldrich, IGEPAL® CA-630, I3021), with 2 mM PMSF and proteinase inhibitor cocktail (Sigma-Aldrich, cOmplete™, 11836170001). Lysates were cleared by centrifugation at 13,000 g for 30 min at 4°C. Total protein concentration was measured using the Bio-Rad Protein Assay (500-0006). Samples were resolved by 12% SDS-PAGE followed by western blotting with anti-RFP (rabbit; 1:1,000; Clontech, R10367), or anti-GFP (rabbit; 1:5,000; Invitrogen Molecular Probes, A6455). Secondary antibody was anti-rabbit (1:20,000; HiSec™ HRP-conjugated, Ab202) followed by detection using the SuperSignal West Pico Chemiluminescent substrate (Pierce, 34080). Atg7 acetylation was assessed by immunoblot with RFP-Trapped (Chromotek RFP-Trap®\_A,

**Table 3.** Oligonucleotide primers used for plasmid construction in this study.

Gene (Locus)	Description	Enzyme sites	Primer sequence
<i>GCN5</i> (MGG_03677)	Deletion construct	—	5'-AATGTGAATTCGAACACAAAACGTTTCAG-3'
		—	5'-GGAACGGGATCCCGTGCTATCTCGTTGGG-3'
	GFP-tagging (N-terminal) under <i>RP27</i> promoter	<i>PstI</i>	5'-GACTGTTCTGCAGTTTGTGACCCATTTGTACATGAT-3'
		<i>HindIII</i>	5'-GAGTGTAAAGCTTCTAGGCGTCCGGATCACAGTGCAT-3'
		<i>BamHI</i>	5'-GAGAGTGGATCCATAAATGTAGGTATTACTCTGA-3'
		<i>NcoI</i>	5'-GAGAGTGACCATGGTTGAAGATTGGGTTCTACGA-3'
		<i>NcoI</i>	5'-GAGAGTGACCATGGTGAGCAAGGGCAGGAGCTGT-3'
		<i>KpnI</i>	5'-GAGAGTGAGGTACCCTTGACAGCTCGTCCATGCCGAG-3'
	mCherry-tagging (C-terminal)	<i>KpnI</i>	5'-GAGAGTGAGGTACCCTTGACAGCTCGTCCATGCCGAG-3'
		<i>EcoRI</i>	5'-GTGTGAATCTGCGCATTAAAGTCATGGTTCAAGATGTGA-3'
		<i>EcoRI</i>	5'-GTGTGAATTCGAGGCGCGCACCATTAATGCAGTGA-3'
		<i>NdeI</i>	5'-GGAATTCATATGTGGTCAAGATGTGACCACTCGGGG-3'
<i>NdeI</i>		5'-GGAATTCATATGAAGGGCGAGGAGGATAACATGG-3'	
<i>BamHI</i>		5'-GTGTGGATCCCTACTGTACAGCTCGTCCATGCCG-3'	
Complementation	<i>EcoRI</i>	5'-GAGTGAAGTTCGTTTCAGTTTCGGGAAATCCTAACGCC-3'	
	<i>KpnI</i>	5'-AGAGTGAGGTACCCTCAACCAACTATATGCATGTTCTCAAAGCCGAC-3'	
	<i>EcoRI</i>	5'-GTGTGAATTCGAAGCTCCAGATACAGAGGTTCTGT-3'	
<i>ATG1</i> (MGG_06393)	Deletion construct	<i>BamHI</i>	5'-GTGTGGATCCCTCAACCGGATTGTTTCATCTT-3'
		<i>PstI</i>	5'-GTGTCTGCAGAACGCGAGACGTTGGCCCTAA-3'
	dsRed-tagging (C-terminal), under <i>RP27</i> promoter	<i>HindIII</i>	5'-GTGTAAAGCTTAAGCCTCCAGATACAGAGGTTCTGT-3'
		<i>NcoI</i>	5'-AACCCAACTTCAAACCATGGGAAATGATGAGCGCGCCG-3'
		<i>EcoRI</i>	5'-CTATGACATGATTACGAATTCGAAGCATCTACCATCCCTTC-3'
<i>ATG7</i> (MGG_07297)	dsRed-tagging (C-terminal), under <i>RP27</i> promoter	<i>EcoRI</i>	5'-CCGAATTCATGGACAACACCGAGGACGTCATCAAG-3'
		<i>EcoRI</i>	5'-CCGGAATTCGAAACGCGTTTTATTCTTGTGACATGGAGCTATTAATCACTAC
		<i>EcoRI</i>	TGGGAGCCGGAGTGCGGG-3'

rta-100) proteins, against the anti-acetyl lysine (anti-acK) (Abcam, ab61257) antibody. Total lysates from the GFP-Gcn5 strain was subject to immunoprecipitation with GFP-Trap (Chromo Tek, gta-20). The IP proteins were then identified by mass spectrometry (Q Exactive, Thermo Finnigan, US).

### Mass spectrometry

Gcn5-IP proteins (about 30 µg) were in-solution digested using trypsin (Sigma-Aldrich, T7409) for 20 h at 37°C, and the digested peptides were subject to Nano-HPLC/ESI-ion trap-MS/MS analysis with Q exactive (Thermo Finnigan, US). Raw MS data files were processed and analyzed using Mascot2.2 (Matrix Science, UK). The database search was performed with the following parameters: Database: uniprot; Taxonomy: *Magnaporthe oryzae* (39372); Enzyme: Trypsin; Dynamical modifications: Oxidation (M); Fixed modifications: Carbamidomethyl (C); Max Missed Cleavages: 2; ProteomicsTools: 3.1.6; Filter by score > = 20.

For identification of acetylated proteins and sites from *GCN5OX* and *gcn5Δ* mutants, total lysates (10 mg) from each strain were digested with trypsin for 20 h at 37°C, followed by enrichment of acetylated peptides with PTMScan Acetyl-Lysine Motif (acK) Kit (Cell Signaling Technology, 13416S). The peptides were separated on Easy-nLC1000 (Thermo Fisher Scientific Inc., Waltham, MA, US) with trap columns (EASY column SC001 traps 150 µm\*20 mm [RP-C18]) and analysis column (EASY column SC200 150 µm\*100 mm [RP-C18]). The peptides analyzed with Q exactive (Thermo Finnigan, US), eluted from the column with a linear solvent gradients (A: 0.1% formic acid [FA] 2% ACN; B: 84% ACN/0.1% FA) for 120 min at a flow rate of 300 nL/min (110 min of gradient from 0 to 45% buffer B; 8 min gradient from 45 to 100% buffer B; 2 min of

100% buffer B). This LC gradient was used for all mobile phase compositions. The mass spectrometer was operated in the positive ion mode at 2 kV and the capillary temperature was set to 180°C. The full scan was performed with enhanced mode, 350 to 1800 m/z. Raw LCMS/MS data files were processed with Maxquant software (version 1.3.0.5) for database searching, using uniprot\_Magnaporthe\_oryzae\_39372\_20160315.fasta, and with the following parameters: Main search ppm: 6; Missed cleavage: 4; MS/MS tolerance ppm: 20; De-Isotopic: TRUE; enzyme: Trypsin; Fixed modification: Carbamidomethyl (C); Variable modification: Oxidation (M), Acetyl (Protein N-term), Avetyl (K); Decoy database pattern: reverse; iBAQ: TRUE; Match between runs: 2 min; Peptide FDR: 0.01; Protein FDR: 0.01. Protein or peptide matching and annotation were performed with Perseus (version 1.3.0.4). The Mass Spectrometry analysis was performed by Shanghai Applied Protein Technology Co. Ltd. (<http://www.apptbiotech.com/>).

### Statistical analysis

For quantification of radial growth or conidia production, 3 biological repeats were performed for calculation of average value and standard deviation. P value was calculated with TTEST function in Excel (Microsoft office 2007) with the setting as Two-Sample Assuming Unequal Variances.

### Abbreviations

ATG genes	autophagy-related genes
DAPI	4',6-diamidino-2-phenylindole
DIC	differential interference contrast
HAT	histone acetyltransferase
IP	immunoprecipitation or immunoprecipitated

LREs	light responsive elements
NAT	N-terminal acetyltransferase
PAS	phagophore assembly site

## Disclosure of potential financial interests

The authors declare they have no competing financial interests.

## Acknowledgments

We are grateful to Ziwei Qu (Temasek Life Sciences Laboratory, Singapore) for construction of the plasmids for *GCN5* knockout and overexpression, and Fan Yang for construction of the vector pFGL820 and pFGL821. We thank the Shanghai Applied Protein Technology Co. Ltd for technology support in mass spectrometry identification of immunoprecipitated proteins and acetylated peptides/residues.

## Funding

This work was supported by the National Basic Research Program of China (973 Program, grant number 2015CB150600) and the National Research Foundation, Singapore (Prime Minister's Office, NRF-CRP7-2010-02).

## References

- Talbot NJ. On the trail of a cereal killer: Exploring the biology of *magnaporthe grisea*. *Annu Rev Microbiol* 2003; 57:177-202; PMID:14527276; <https://doi.org/10.1146/annurev.micro.57.030502.090957>
- Lee K, Singh P, Chung WC, Ash J, Kim TS, Hang L, Park S. Light regulation of asexual development in the rice blast fungus, *magnaporthe oryzae*. *Fungal Genet Biol* 2006; 43:694-706; PMID:16765070; <https://doi.org/10.1016/j.fgb.2006.04.005>
- Talbot NJ. Having a blast: Exploring the pathogenicity of *magnaporthe grisea*. *Trends Microbiol* 1995; 3:9-16; PMID:7719639; [https://doi.org/10.1016/S0966-842X\(00\)88862-9](https://doi.org/10.1016/S0966-842X(00)88862-9)
- Liu XH, Lu JP, Zhang L, Dong B, Min H, Lin FC. Involvement of a *Magnaporthe grisea* serine/threonine kinase gene, *MgATG1*, in appressorium turgor and pathogenesis. *Eukaryot Cell* 2007; 6:997-1005; PMID:17416896; <https://doi.org/10.1128/EC.00011-07>
- Liu TB, Liu XH, Lu JP, Zhang L, Min H, Lin FC. The cysteine protease *MoAtg4* interacts with *MoAtg8* and is required for differentiation and pathogenesis in *Magnaporthe oryzae*. *Autophagy* 2010; 6:74-85; PMID:19923912; <https://doi.org/10.4161/auto.6.1.10438>
- Lu JP, Liu XH, Feng XX, Min H, Lin FC. An autophagy gene, *MgATG5*, is required for cell differentiation and pathogenesis in *Magnaporthe oryzae*. *Curr Genet* 2009; 55:461-73; PMID:19629489; <https://doi.org/10.1007/s00294-009-0259-5>
- Veneault-Fourrey C, Barooah M, Egan M, Wakley G, Talbot NJ. Autophagic fungal cell death is necessary for infection by the rice blast fungus. *Science* 2006; 312:580-3; PMID:16645096; <https://doi.org/10.1126/science.1124550>
- Deng YZ, Ramos-Pamplona M, Naqvi NI. Autophagy-assisted glyco-gen catabolism regulates asexual differentiation in *magnaporthe oryzae*. *Autophagy* 2009; 5:33-43; PMID:19115483; <https://doi.org/10.4161/auto.5.1.7175>
- Dong B, Liu XH, Lu JP, Zhang FS, Gao HM, Wang HK, Lin FC. *MgAtg9* trafficking in *magnaporthe oryzae*. *Autophagy* 2009; 5:946-53; PMID:19556868; <https://doi.org/10.4161/auto.5.7.9161>
- He Y, Deng YZ, Naqvi NI. *Atg24*-assisted mitophagy in the foot cells is necessary for proper asexual differentiation in *Magnaporthe oryzae*. *Autophagy* 2013; 9:1818-27; PMID:23958498; <https://doi.org/10.4161/auto.26057>
- He M, Kernshaw MJ, Soanes DM, Xia Y, Talbot NJ. Infection-associated nuclear degeneration in the rice blast fungus *magnaporthe oryzae* requires non-selective macro-autophagy. *PLoS One* 2012; 7(3): e33270; PMID:22448240; <https://doi.org/10.1371/journal.pone.0033270>
- Liu Y, Schiff M, Czymbek K, Tallóczy Z, Levine B, Dinesh-Kumar SP. Autophagy regulates programmed cell death during the plant innate immune response. *Cell* 2005; 121:567-77; PMID:15907470; <https://doi.org/10.1016/j.cell.2005.03.007>
- Noda T, Ohsumi Y. Tor, a phosphatidylinositol kinase homologue, controls autophagy in yeast. *J Biol Chem* 1998; 273:3963-6; PMID:9461583; <https://doi.org/10.1074/jbc.273.7.3963>
- Dementhon K, Saupe SJ, Clave C. Characterization of *IDI-4*, a bZIP transcription factor inducing autophagy and cell death in the fungus *podospora anserina*. *Mol Microbiol* 2004; 53:1625-40; PMID:15341644; <https://doi.org/10.1111/j.1365-2958.2004.04235.x>
- Klionsky DJ, Cregg JM, Dunn WA Jr, Emr SD, Sakai Y, Sandoval IV, Sibirny A, Subramani S, Thumm M, Veenhuis M, et al. A unified nomenclature for yeast autophagy-related genes. *Dev Cell* 2003; 5:539-45; PMID:14536056; [https://doi.org/10.1016/S1534-5807\(03\)00296-X](https://doi.org/10.1016/S1534-5807(03)00296-X)
- Klionsky DJ. Autophagy: from phenomenology to molecular understanding in less than a decade. *Nat Rev Mol Cell Biol* 2007; 8:931-7; PMID:17712358; <https://doi.org/10.1038/nrm2245>
- Yao Z, Delorme-Axford E, Backues SK, Klionsky DJ. *Atg41/Icy2* regulates autophagosome formation. *Autophagy* 2015; 11:2288-99; PMID:26565778; <https://doi.org/10.1080/15548627.2015.1107692>
- Ichimura Y, Kirisako T, Takao T, Satomi Y, Shimonishi Y, Ishihara N, Mizushima N, Tanida I, Kominami E, Ohsumi M, et al. A ubiquitin-like system mediates protein lipidation. *Nature* 2000; 408:488-92; PMID:11100732; <https://doi.org/10.1038/35044114>
- Kabeya Y, Mizushima N, Ueno T, Yamamoto A, Kirisako T, Noda T, Kominami E, Ohsumi Y, Yoshimori T. *LC3*, a mammalian homologue of yeast *Apg8p*, is localized in autophagosomal membranes after processing. *EMBO J* 2000; 19:5720-8; PMID:11060023; <https://doi.org/10.1093/emboj/19.21.5720>
- Kirisako T, Baba M, Ishihara N, Miyazawa K, Ohsumi M, Yoshimori T, Noda T, Ohsumi Y. Formation process of autophagosome is traced with *Apg8/Aut7p* in yeast. *J Cell Biol* 1999; 147:435-46; PMID:10525546; <https://doi.org/10.1083/jcb.147.2.435>
- Yi C, Ma M, Ran L, Zheng J, Tong J, Zhu J, Ma C, Sun Y, Zhang S, Feng W, et al. Function and molecular mechanism of acetylation in autophagy regulation. *Science* 2012; 336:474-7; PMID:22539722; <https://doi.org/10.1126/science.1216990>
- Lin SY, Li TY, Liu Q, Zhang C, Li X, Chen Y, Zhang SM, Lian G, Liu Q, Ruan K, et al. *GSK3-TIP60-ULK1* signaling pathway links growth factor deprivation to autophagy. *Science* 2012; 336:477-81; PMID:22539723; <https://doi.org/10.1126/science.1217032>
- Lin SY, Li TY, Liu Q, Zhang C, Li X, Chen Y, Zhang SM, Lian G, Liu Q, Ruan K, et al. Protein phosphorylation-acetylation cascade connects growth factor deprivation to autophagy. *Autophagy* 2012; 8:1385-6; PMID:22717509; <https://doi.org/10.4161/auto.20959>
- Deng YZ, Qu Z, Naqvi NI. Twilight, a novel circadian-regulated gene, integrates phototropism with nutrient and redox homeostasis during fungal development. *PLoS Pathog* 2015; 11:e1004972; PMID:26102503; <https://doi.org/10.1371/journal.ppat.1004972>
- Imhof A, Yang XJ, Ogryzko VV, Nakatani Y, Wolffe AP, Ge H. Acetylation of general transcription factors by histone acetyltransferases. *Curr Biol* 1997; 7:689-92; PMID:9285713; [https://doi.org/10.1016/S0960-9822\(06\)00296-X](https://doi.org/10.1016/S0960-9822(06)00296-X)
- Hu Z, Song N, Zheng M, Liu X, Liu Z, Xing J, Ma J, Guo W, Yao Y, Peng H, et al. Histone acetyltransferase *GCN5* is essential for heat stress-responsive gene activation and thermotolerance in *Arabidopsis*. *Plant J* 2015; 84:1178-91; PMID:26576681; <https://doi.org/10.1111/tpl.13076>
- Moraga F, Aquea F. Composition of the SAGA complex in plants and its role in controlling gene expression in response to abiotic stresses. *Front Plant Sci* 2015; 6:865; PMID:26528322; <https://doi.org/10.3389/fpls.2015.00865>
- Wang Z, Cao H, Chen F, Liu Y. The roles of histone acetylation in seed performance and plant development. *Plant Physiol Biochem* 2014; 84:125-33; PMID:25270163; <https://doi.org/10.1016/j.plaphy.2014.09.010>

- [29] Qiu H, Chereji RV, Hu C, Cole HA, Rawal Y, Clark DJ, Hinnebusch AG. Genome-wide cooperation by HAT Gcn5, remodeler SWI/SNF, and chaperone Ydj1 in promoter nucleosome eviction and transcriptional activation. *Genome Res* 2016; 26:211-25; PMID:26602697; <https://doi.org/10.1101/gr.196337.115>
- [30] Gaupel AC, Begley TJ, Tenniswood M. Gcn5 modulates the cellular response to oxidative stress and histone deacetylase inhibition. *J Cell Biochem* 2015; 116:1982-92; PMID:25755069; <https://doi.org/10.1002/jcb.25153>
- [31] Xie L, Zeng J, Luo H, Pan W, Xie J. The roles of bacterial GCN5-related N-acetyltransferases. *Crit Rev Eukaryot Gene Expr* 2014; 24:77-87; PMID:24579671; <https://doi.org/10.1615/CritRevEukaryotGeneExpr.2014007988>
- [32] Greene NP, Crow A, Hughes C, Koronakis V. Structure of a bacterial toxin-activating acyltransferase. *Proc Natl Acad Sci U S A* 2015; 112:E3058-66; PMID:26016525; <https://doi.org/10.1073/pnas.1503832112>
- [33] Yin YW, Jin HJ, Zhao W, Gao B, Fang J, Wei J, Zhang DD, Zhang J, Fang D. The histone acetyltransferase GCN5 expression is elevated and regulated by c-Myc and E2F1 transcription factors in human colon cancer. *Gene Expr* 2015; 16:187-96; PMID:26637399; <https://doi.org/10.3727/105221615X14399878166230>
- [34] Dekker FJ, Haisma HJ. Histone acetyl transferases as emerging drug targets. *Drug Discov Today* 2009; 14:942-8; PMID:19577000; <https://doi.org/10.1016/j.drudis.2009.06.008>
- [35] Tsukada M, Ohsumi Y. Isolation and characterization of autophagy-defective mutants of *saccharomyces cerevisiae*. *FEBS Lett* 1993; 333:169-74; PMID:8224160; [https://doi.org/10.1016/0014-5793\(93\)80398-E](https://doi.org/10.1016/0014-5793(93)80398-E)
- [36] Tanida I, Ueno T, Kominami E. LC3 conjugation system in mammalian autophagy. *Int J Biochem Cell Biol* 2004; 36:2503-18; PMID:15325588; <https://doi.org/10.1016/j.biocel.2004.05.009>
- [37] Park SC, Kwon HB, Shih MC. Cis-acting elements essential for light regulation of the nuclear gene encoding the a subunit of chloroplast glyceraldehyde 3-phosphate dehydrogenase in *arabidopsis thaliana*. *Plant Physiol* 1996; 112:1563-71; PMID:8972600; <https://doi.org/10.1104/pp.112.4.1563>
- [38] Takanaka Y, Okano T, Yamamoto K, Fukada Y. A negative regulatory element required for light-dependent pinopsin gene expression. *J Neurosci* 2002; 22:4357-63; PMID:12040041; <https://doi.org/20026417>
- [39] Kikuchi H, Kuribayashi F, Takami Y, Imajoh-Ohmi S, Nakayama T. GCN5 regulates the activation of PI3K/Akt survival pathway in B cells exposed to oxidative stress via controlling gene expressions of Syk and Btk. *Biochem Biophys Res Commun* 2011; 405:657-61; PMID:21281601; <https://doi.org/10.1016/j.bbrc.2011.01.088>
- [40] O'Meara TR, Hay C, Price MS, Giles S, Alspaugh JA. *Cryptococcus neoformans* histone acetyltransferase Gcn5 regulates fungal adaptation to the host. *Eukaryot Cell* 2010; 9:1193-1202; PMID:20581290; <https://doi.org/10.1128/EC.00098-10>
- [41] Guo R, Chen J, Mitchell DL, Johnson DG. GCN5 and E2F1 stimulate nucleotide excision repair by promoting H3K9 acetylation at sites of damage. *Nucleic Acids Res* 2011; 39:1390-7; PMID:20972224; <https://doi.org/10.1093/nar/gkq983>
- [42] Mizuguchi G, Vassilev A, Tsukiyama T, Nakatani Y, Wu C. ATP-dependent nucleosome remodeling and histone hyperacetylation synergistically facilitate transcription of chromatin. *J Biol Chem* 2001; 276:14773-83; PMID:11279013; <https://doi.org/10.1074/jbc.M100125200>
- [43] Strenkert D, Schmollinger S, Sommer F, Schulz-Raffelt M, Schroda M. Transcription factor-dependent chromatin remodeling at heat shock and copper-responsive promoters in *chlamydomonas reinhardtii*. *Plant Cell* 2011; 23:2285-301; PMID:21705643; <https://doi.org/10.1105/tpc.111.085266>
- [44] Tscherner M, Zwolanek F, Jenull S, Sedlazeck FJ, Petryshyn A, Frohner IE, Mavrianos J, Chauhan N, von Haeseler A, Kuchler K. The *Candida albicans* histone acetyltransferase Hat1 regulates stress resistance and virulence via distinct chromatin assembly pathways. *PLoS Pathog* 2015; 11:e1005218; PMID:26473952; <https://doi.org/10.1371/journal.ppat.1005218>
- [45] Chang P, Fan X, Chen J. Function and subcellular localization of Gcn5, a histone acetyltransferase in *Candida albicans*. *Fungal Genet Biol* 2015; 81:132-41; PMID:25656079; <https://doi.org/10.1016/j.fgb.2015.01.011>
- [46] Gonzalez-Prieto JM, Rosas-Quijano R, Dominguez A, Ruiz-Herrera J. The UmGcn5 gene encoding histone acetyltransferase from *Ustilago maydis* is involved in dimorphism and virulence. *Fungal Genet Biol* 2014; 71:86-95; PMID:25242418; <https://doi.org/10.1016/j.fgb.2014.09.002>
- [47] Lee IH, Finkel T. Regulation of autophagy by the p300 acetyltransferase. *J Biol Chem* 2009; 284:6322-8; PMID:19124466; <https://doi.org/10.1074/jbc.M807135200>
- [48] Sebti S, Prébois C, Pérez-Gracia E, Bauvy C, Desmots F, Pirot N, Gongora C, Bach AS, Hubberstey AV, Palissot V, et al. BAT3 modulates p300-dependent acetylation of p53 and autophagy-related protein 7 (ATG7) during autophagy. *Proc Natl Acad Sci U S A* 2014; 111:4115-20; PMID:24591579; <https://doi.org/10.1073/pnas.1313618111>
- [49] Lee IH, Cao L, Mostoslavsky R, Lombard DB, Liu J, Bruns NE, Tsokos M, Alt FW, Finkel T. A role for the NAD-dependent deacetylase Sirt1 in the regulation of autophagy. *Proc Natl Acad Sci U S A* 2008; 105:3374-9; PMID:18296641; <https://doi.org/10.1073/pnas.0712145105>
- [50] Muzaffar S, Bose C, Banerji A, Nair BG, Chattoo BB. Anacardic acid induces apoptosis-like cell death in the rice blast fungus *magnaporthe oryzae*. *Appl Microbiol Biotechnol* 2016; 100:323-35; PMID:26381667; <https://doi.org/10.1007/s00253-015-6915-4>
- [51] Sun Y, Jiang X, Chen S, Price BD. Inhibition of histone acetyltransferase activity by anacardic acid sensitizes tumor cells to ionizing radiation. *FEBS Lett* 2006; 580:4353-6; PMID:16844118; <https://doi.org/10.1016/j.febslet.2006.06.092>
- [52] Seong YA, Shin PG, Yoon JS, Yadunandam AK, Kim GD. Induction of the endoplasmic reticulum stress and autophagy in human lung carcinoma A549 cells by anacardic acid. *Cell Biochem Biophys* 2014; 68:369-77; PMID:23955513; <https://doi.org/10.1007/s12013-013-9717-2>
- [53] Eisenberg T, Schroeder S, Büttner S, Carmona-Gutierrez D, Pendl T, Andryushkova A, Mariño G, Pietrocola F, Harger A, Zimmermann A, et al. A histone point mutation that switches on autophagy. *Autophagy* 2014; 10:1143-5; PMID:24879160; <https://doi.org/10.4161/auto.28767>
- [54] Venters BJ, Wachi S, Mavrich TN, Andersen BE, Jena P, Sinnamon AJ, Jain P, Rolleri NS, Jiang C, Hemeryck-Walsh C, et al. A comprehensive genomic binding map of gene and chromatin regulatory proteins in *saccharomyces*. *Mol Cell* 2011; 41:480-92; PMID:21329885; <https://doi.org/10.1016/j.molcel.2011.01.015>
- [55] Abate G, Bastonini E, Braun KA, Verdone L, Young ET, Caserta M. Snf1/AMPK regulates Gcn5 occupancy, H3 acetylation and chromatin remodeling at *S. cerevisiae* ADY2 promoter. *Biochim Biophys Acta* 2012; 1819:419-27; PMID:22306658; <https://doi.org/10.1016/j.bbagr.2012.01.009>
- [56] Hickman MJ, Spatt D, Winston F. The Hog1 mitogen-activated protein kinase mediates a hypoxic response in *saccharomyces cerevisiae*. *Genetics* 2011; 188:325-38; PMID:21467572; <https://doi.org/10.1534/genetics.111.128322>
- [57] Ramos-Pamplona M, Naqvi NI. Host invasion during rice-blast disease requires carnitine-dependent transport of peroxisomal acetyl-CoA. *Mol Microbiol* 2006; 61:61-75; PMID:16824095; <https://doi.org/10.1111/j.1365-2958.2006.05194.x>
- [58] Talbot NJ, Ebbole DJ, Hamer JE. Identification and characterization of MPG1, a gene involved in pathogenicity from the rice blast fungus *magnaporthe grisea*. *Plant Cell* 1993; 5:1575-90; PMID:8312740; <https://doi.org/10.1105/tpc.5.11.1575>
- [59] Deng YZ, Qu Z, He Y, Naqvi NI. Sorting nexin Snx41 is essential for conidiation and mediates glutathione-based antioxidant defense during invasive growth in *magnaporthe oryzae*. *Autophagy* 2012; 8:1058-70; PMID:22561104; <https://doi.org/10.4161/auto.20217>